nature structural & molecular biology

A phospho-BAD BH3 helix activates glucokinase by a mechanism distinct from that of allosteric activators

Benjamin Szlyk[1,7], Craig R Braun[2,7], Sanda Ljubicic[1,3], Elaura Patton[1], Gregory H Bird[2], Mayowa A Osundiji[1], Franz M Matschinsky[4], Loren D Walensky[2,5,6] & Nika N Danial[1,3]

Glucokinase (GK) is a glucose-phosphorylating enzyme that regulates insulin release and hepatic metabolism, and its loss of function is implicated in diabetes pathogenesis. GK activators (GKAs) are attractive therapeutics in diabetes; however, clinical data indicate that their benefits can be offset by hypoglycemia, owing to marked allosteric enhancement of the enzyme's glucose affinity. We show that a phosphomimetic of the BCL-2 homology 3 (BH3) α-helix derived from human BAD, a GK-binding partner, increases the enzyme catalytic rate without dramatically changing glucose affinity, thus providing a new mechanism for pharmacologic activation of GK. Remarkably, BAD BH3 phosphomimetic mediates these effects by engaging a new region near the enzyme's active site. This interaction increases insulin secretion in human islets and restores the function of naturally occurring human GK mutants at the active site. Thus, BAD phosphomimetics may serve as a new class of GKAs.

Loss of glycemic control in type 2 diabetes (T2D) is the outcome of combined defects in insulin action and insulin secretion, both of which have strong genetic and environmental components[1,2]. A major challenge in T2D therapy is to achieve durable glycemic control while minimizing side effects and the risk of hypoglycemia[3]. Small-molecule GKAs are among multiple investigational agents currently under development for their glucose-lowering capacity in T2D[4,5]. GK (hexokinase IV) is a key component of the mammalian glucose-sensing machinery with tissue-specific roles in insulin secretion by β-cells, glucose utilization and storage in hepatocytes, central glucose sensing and counter-regulatory responses to hypoglycemia[5]. As compared to those of other hexokinase isoforms, unique kinetic properties of GK, such as lack of product inhibition, a high $S_{0.5}$ (K_m) value for glucose and positive substrate cooperativity, render it particularly well suited for regulation of blood glucose levels. As such, gain-of-function mutations in GK are central to the molecular pathogenesis of persistent hyperinsulinemic hypoglycemia of infancy, whereas loss-of-function mutations in the enzyme are linked to maturity-onset diabetes of the young type 2 (MODY2) and permanent neonatal diabetes mellitus[5]. Beyond the fundamental relevance of GK in β-cell function, emerging evidence also suggests that increased GK activity and glucose metabolism in these cells can impart mitogenic and prosurvival benefits, thus leading to β-cell mass expansion[6]. Improvement of both β-cell function and mass through increased GK activity may well expand the potential utility of synthetic GKAs beyond T2D to restoration and maintenance of functional β-cell mass for the treatment of type 1 diabetes (T1D).

All GKAs reported to date bind to the allosteric site in the enzyme, which is located 20 Å from its active site, and markedly increase the affinity of the enzyme for glucose, typically from 7–8 mM to approximately 1–2 mM (refs. 4,5). Structural analysis of several GK conformations in the presence and absence of glucose and GKAs has provided insights into the mechanism of its enzymatic action[7–14]. Although the precise transitions between GK conformations are still under active investigation, several studies indicate that, in the presence of increasing glucose concentrations, GK transitions from an inactive super-open conformation with low affinity for glucose to an active closed conformation that is catalytically competent for binding of substrates and release of products[7–11,13–16]. Gain-of-function mutations in GK, which typically cluster in the allosteric site, and binding of allosteric GKAs to this region cause this transition to occur at lower glucose concentrations[5]. Although several allosteric activators of GK have shown promising short-term effects, a drawback of these compounds is the risk of development of hypoglycemia over time[3,17–19], thus warranting an exploration of alternative pharmacologic modalities for GK activation, particularly of those with a more tempered effect on glucose affinity[5].

The BCL-2 family protein BAD binds GK and regulates glucose metabolism in the liver and β-cells[20–23]. BAD belongs to the BH3-only subclass of proapoptotic BCL-2 family proteins, which share sequence homology only within an α-helical BH3 domain. Using mutational studies, mouse models and genetic reconstitution assays, we have shown that BAD phosphorylation on a conserved serine residue within its BH3 domain, Ser155 in mouse BAD corresponding to Ser118 in the human sequence, acts as a molecular switch that enables

[1]Department of Cancer Biology, Dana-Farber Cancer Institute, Boston, Massachusetts, USA. [2]Department of Pediatric Oncology, Dana-Farber Cancer Institute, Boston, Massachusetts, USA. [3]Department of Cell Biology, Harvard Medical School, Boston, Massachusetts, USA. [4]Department of Biochemistry and Biophysics, University of Pennsylvania School of Medicine, Philadelphia, Pennsylvania, USA. [5]Department of Biological Chemistry and Molecular Pharmacology, Harvard Medical School, Boston, Massachusetts, USA. [6]Department of Pediatric Oncology, Children's Hospital, Boston, Massachusetts, USA. [7]These authors contributed equally to this work. Correspondence should be addressed to L.D.W. (loren_walensky@dfci.harvard.edu) or N.N.D. (nika_danial@dfci.harvard.edu).

Received 11 August; accepted 15 October; published online 8 December 2013; doi:10.1038/nsmb.2717

Table 1 Modulation of glucokinase kinetic parameters by BAD BH3 stapled peptides

Treatment	$S_{0.5}$ (mM)	V_{max} (% veh)	n_H	$S_{0.5\ veh}/S_{0.5\ treat}$	
Vehicle	7.49 ± 0.18	100	1.61 ± 0.03	1.00 ± 0.05	$n = 18$
GKA (RO0281675)	1.62 ± 0.13***	138 ± 6.15***	1.71 ± 0.06	4.62 ± 0.47***	$n = 6$
BAD $SAHB_A$ (S118D)	6.54 ± 0.15**	144 ± 4.64***	1.71 ± 0.03	1.15 ± 0.05	$n = 18$
BAD $SAHB_A$ (S118pS)	6.00 ± 0.68**	129 ± 6.54**	1.69 ± 0.18	1.25 ± 0.17	$n = 3$
BAD $SAHB_A$ (S118L)	8.14 ± 0.41	89.6 ± 5.01	1.62 ± 0.05	0.92 ± 0.07	$n = 7$
BAD $SAHB_A$ (S118D) + GKA	1.35 ± 0.07***	124 ± 1.54*	1.84 ± 0.07*	5.55 ± 0.41***	$n = 4$

Kinetic parameters were derived with the Hill equation as described in Online Methods. $S_{0.5\ veh}/S_{0.5\ treat}$ in the fourth column calculates the fold change in glucose affinity resulting from each treatment. Data represent means ± s.e.m. For each kinetic parameter, four simultaneous comparisons were made with one-way ANOVA (Online Methods). *$P < 0.05$; **$P < 0.01$; ***$P < 0.001$ compared with vehicle control (veh).

it to enhance glucose metabolism and support insulin secretion in β-cells[22]. Concomitant with these metabolic benefits, phosphorylation of the BH3 domain blocks BAD's capacity to engage the prosurvival proteins BCL-2, BCL-X_L and BCL-W and thereby neutralizes its proapoptotic function[20,22]. Importantly, BAD phosphorylation is sensitive to glucose, nutritional (fed and fasted) states and hormones or growth factors known to regulate metabolic adaptations to nutritional states, thus suggesting that BAD phosphorylation and its functional cross-talk with GK may serve as a homeostatic sensor of the nutrient milieu (reviewed in ref. 20).

The BAD BH3 domain is not only required but also sufficient to mimic BAD's ability to influence GK, as evidenced by the capacity of stabilized α-helices of BCL-2 domains (SAHBs) modeled after the phospho-BH3 helix of BAD to activate GK and restore insulin secretion in BAD-deficient islets[22]. However, the region of GK engaged by the BAD BH3 domain and the mechanism of enzyme activation was not known. Hydrocarbon-stapled peptides that recapitulate the natural structure of bioactive helices have proven to be both powerful tools for dissecting signaling pathways and prototype therapeutics for targeting protein interactions[22,24–26]. Given the functional link between phospho-BAD BH3 and GK[22], we set out to investigate the molecular and structural properties of BAD SAHBs as synthetic GKAs. Here, we define the enzymatic and structural characteristics of GK bound to the BAD phospho-BH3 helix and demonstrate previously unanticipated fundamental mechanistic distinctions from allosteric GKAs. Thus, phospho-BAD BH3 mimetics may represent a new class of synthetic GKAs.

RESULTS

The effect of phospho-BAD mimetic compounds on GK kinetics

To determine how the inherent characteristics of GK are altered by phospho-BAD BH3, we synthesized a panel of stapled peptides modeled after the human BAD BH3 domain for use in kinetic assays with recombinant GK. This panel included the phosphomimic BAD $SAHB_A$ (S118D) and the nonphosphorylatable BAD $SAHB_A$ (S118L) variants (**Supplementary Table 1**). We examined GK activity as a function of the Hill equation in order to evaluate the effect of these stapled peptides on the maximal rate of reaction (V_{max}), the glucose concentration that allows half-maximal activity ($S_{0.5}$) and substrate cooperativity reflected by the sigmoidal response to increasing glucose concentration (Hill coefficient, n_H). We also tested the effect of an archetypal allosteric activator of GK, RO0281675 (ref. 9) for comparison.

The kinetic profile of recombinant GK treated with vehicle (DMSO) or RO0281675 showed good agreement with published data[9] (**Table 1**). Treatment with RO0281675 increased the V_{max}, by approximately 40%, and the affinity for glucose, as reflected by a change in $S_{0.5}$ from 7.49 ± 0.18 mM to 1.62 ± 0.13 mM, with no significant effect on the Hill coefficient (**Table 1**). Similarly, treatment with BAD $SAHB_A$ (S118D) did not change the Hill coefficient but increased the V_{max} by 44%, an increase comparable to that induced by RO0281675 (**Fig. 1a** and **Table 1**). However, treatment with BAD $SAHB_A$ (S118D) resulted in only a minimal change in the $S_{0.5}$ for glucose (6.54 ± 0.15 from 7.49 ± 0.18 mM) despite the substantial increase in V_{max} (**Table 1**). This is markedly different from the observed increase in GK affinity for glucose upon treatment with RO0281675 (**Table 1**).

Mutation of Ser118 to leucine (BAD $SAHB_A$ (S118L)) blunted the capacity of the BAD BH3 helix to activate GK (**Fig. 1a** and **Table 1**), results consistent with the notion that phosphorylation of serine at this site is important for GK activation by BAD[22]. To further examine the effect of Ser118 phosphorylation, we also tested the kinetic profile of GK treated with a phospho-BAD BH3 stapled peptide in which the residue corresponding to Ser118 was replaced with a phosphoserine (BAD $SAHB_A$ (S118pS)) and found that it activates GK in a similar manner to that of BAD $SAHB_A$ (S118D), with minimal effect on glucose affinity or substrate cooperativity (**Table 1**). To our knowledge, this is the first chemical mode of GK activation that has little effect on the $S_{0.5}$ of the enzyme for glucose. This predicts a mechanism of GK activation that is markedly different from that of all allosteric GKAs reported to date[9,10,12,14,15,17,27–32].

Given the distinct modes of GK activation by RO0281675 and BAD $SAHB_A$ (S118D), we next tested their combined effects. Cotreatment with RO0281675 and BAD $SAHB_A$ (S118D) produced changes in glucose affinity that were similar to those of RO0281675 treatment alone, thus indicating that BAD $SAHB_A$ (S118D) does not interfere with RO0281675 binding to the allosteric site (**Fig. 1b** and **Table 1**).

Localization of the phospho-BAD BH3 interaction site on GK

The differences between the modes of GK activation by BAD SAHBs and the allosteric activator RO0281675 predicted distinct binding sites for the two compounds. To identify the interaction site for the phospho-BAD BH3 domain on GK, we generated biotinylated and photoreactive BAD SAHB analogs, further derivatized by phosphorylation at Ser118. This allowed for capture of the covalent BAD $SAHB_A$–GK complex and binding-site analysis by MS/MS sequencing[26,33]. We placed the photoreactive benzoylphenylalanine (Bpa) moiety near

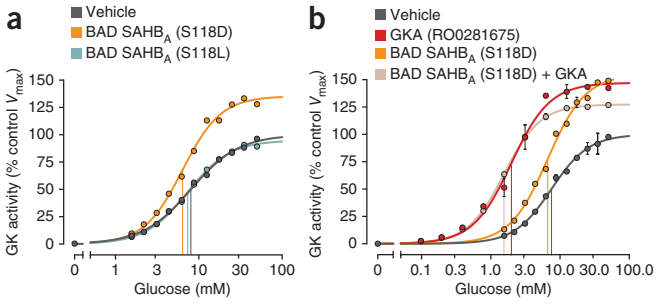

Figure 1 Effects of BAD BH3 stapled peptides on glucokinase (GK) activity. (**a**) GK activity in the presence of BAD $SAHB_A$ (S118D), BAD $SAHB_A$ (S118L) or vehicle alone. (**b**) Activation of GK by BAD $SAHB_A$ (S118D) in the presence or absence of the allosteric GK activator (GKA) RO0281675. Vertical lines in **a** and **b** indicate the glucose concentration corresponding to the $S_{0.5}$ values obtained from the representative experiment shown. Data in **b** show the means and range from a representative experiment. **Table 1** shows a summary and *n* values (3–18 per treatment) for all independent experiments performed similarly.

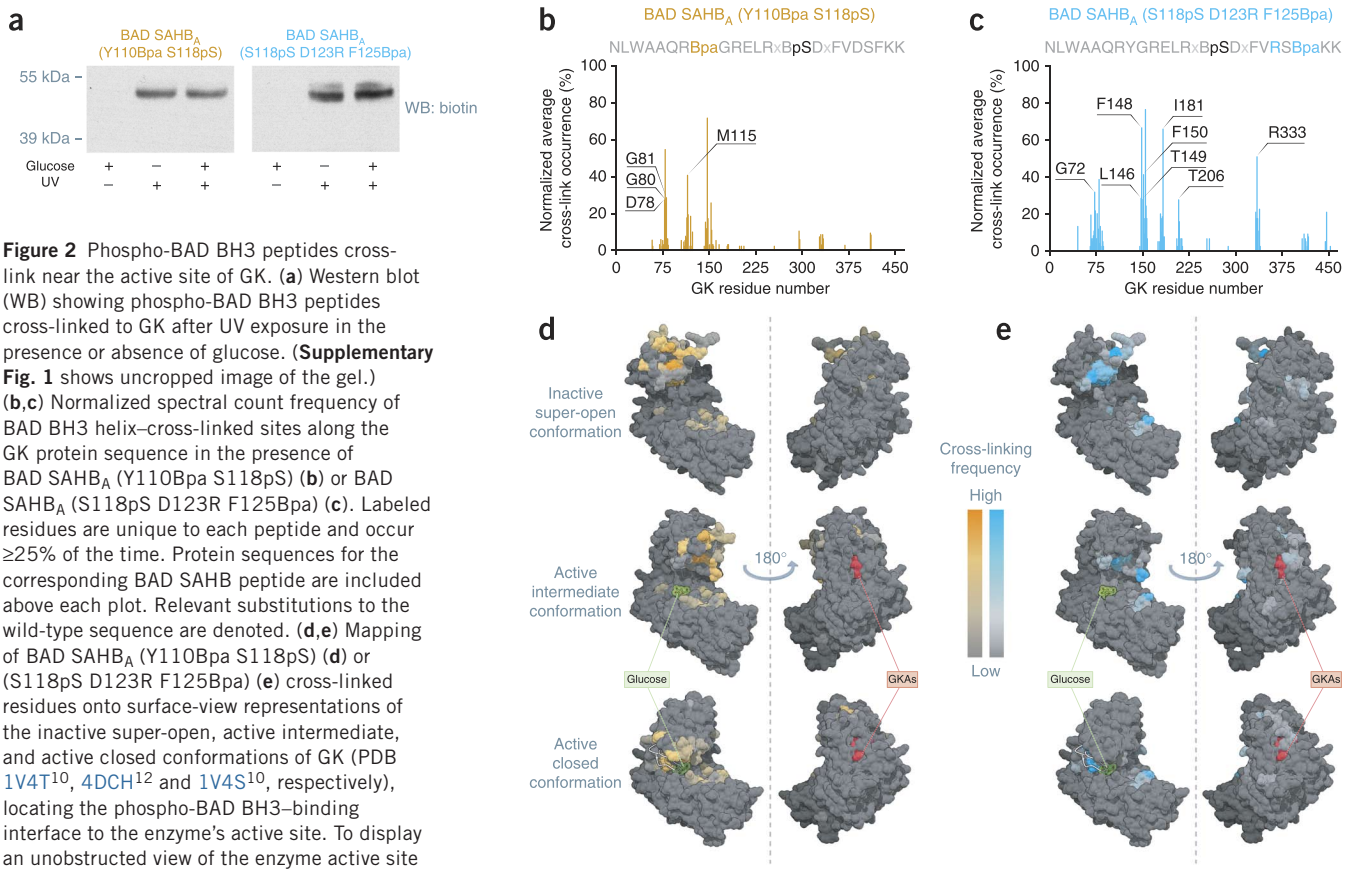

Figure 2 Phospho-BAD BH3 peptides cross-link near the active site of GK. (**a**) Western blot (WB) showing phospho-BAD BH3 peptides cross-linked to GK after UV exposure in the presence or absence of glucose. (**Supplementary Fig. 1** shows uncropped image of the gel.) (**b**,**c**) Normalized spectral count frequency of BAD BH3 helix–cross-linked sites along the GK protein sequence in the presence of BAD SAHB$_A$ (Y110Bpa S118pS) (**b**) or BAD SAHB$_A$ (S118pS D123R F125Bpa) (**c**). Labeled residues are unique to each peptide and occur ≥25% of the time. Protein sequences for the corresponding BAD SAHB peptide are included above each plot. Relevant substitutions to the wild-type sequence are denoted. (**d**,**e**) Mapping of BAD SAHB$_A$ (Y110Bpa S118pS) (**d**) or (S118pS D123R F125Bpa) (**e**) cross-linked residues onto surface-view representations of the inactive super-open, active intermediate, and active closed conformations of GK (PDB 1V4T[10], 4DCH[12] and 1V4S[10], respectively), locating the phospho-BAD BH3–binding interface to the enzyme's active site. To display an unobstructed view of the enzyme active site in the closed structure, the active site loop composed of residues L164–N180 is presented in cartoon form rather than in surface view to show residues located behind the loop. Glucose is shown in green, allosteric GKAs in red and the active site loop in white.

either the N terminus (BAD SAHB$_A$ (Y110Bpa S118pS)) or C terminus (BAD SAHB$_A$ (S118pS D123R F125Bpa)) of the BAD BH3 domain (**Supplementary Table 1**). We further installed a C-terminal tryptic site in BAD SAHB$_A$ (S118pS D123R F125Bpa) by D123R mutagenesis in order to ensure that the resultant Bpa-containing BAD peptide fragment would be sufficiently small for optimal MS/MS sequencing, as previously reported[33]. Importantly, these biotinylated and photoreactive stapled peptides retained their functional interaction with GK, as demonstrated by their capacity to increase the V_{max} while minimally affecting the $S_{0.5}$ for glucose (**Supplementary Table 2**).

Exposure of the BAD SAHB$_A$–GK (2:1) mixtures to UV light led to a cross-linked complex as apparent from biotin western analysis (**Fig. 2a** and **Supplementary Fig. 1**). Importantly, the presence or absence of glucose did not affect the cross-linking of BAD SAHB$_A$–GK complexes (**Fig. 2a** and **Supplementary Fig. 1**). These data predict that the binding site for the phospho-BAD BH3 helix on GK is distinct from the allosteric site, which becomes available only in the presence of glucose[5,10,12,32,34].

We next determined the explicit sites of cross-linking by using MS. We affinity-purified BAD SAHB$_A$–GK covalent adducts by streptavidin pulldown and visualized them as Coomassie-stained SDS-PAGE bands migrating slightly higher than did input protein. After excision and in-gel trypsin digestion, we analyzed the cross-linked adducts by nano-LC-MS/MS[26,33]. We identified Bpa-cross-linked tryptic fragments by searching the MS data for a variable modification corresponding to the mass of the tryptic GK fragment plus the Bpa-containing BAD SAHB$_A$ fragment. We identified the cross-linked amino acids within GK by MS/MS sequencing of the cross-linked peptides and used these MS/MS spectral count frequencies as a measure of the abundance of these modifications (**Fig. 2b**,**c** and **Supplementary Table 3**). Whereas the phospho-BAD peptide with the Bpa moiety closer to the N terminus (BAD SAHB$_A$ (Y110Bpa S118pS)) predominantly cross-linked to GK in the vicinity of M115 (**Fig. 2b**), the photoreactive SAHB with Bpa installed near the C terminus (BAD SAHB$_A$ (S118pS D123R F125Bpa)) uniquely modified the region of GK containing residues I181 (V181 in human GK), T206 and R333 (**Fig. 2c**). In addition, both peptides cross-linked to residues centered around L79 and F150, which lie between the unique interaction sites for each photoreactive BAD SAHB$_A$. Strikingly, mapping of the cross-linked residues onto each of the three previously defined conformational states of GK (PDB 1V4T[10], 4DCH[12] and 1V4S[10]) demonstrates engagement of the phospho-BAD BH3 domain near the active site of the enzyme (**Fig. 2d**,**e**). The interaction surface identified by phospho-BAD peptides is distinct from that of any published GKA. Consistently with this conclusion, there was little observed effect on the cross-linking pattern upon co-incubation of RO0281675 and the photoreactive BAD SAHB$_A$ compounds (**Supplementary Fig. 2**). These data are also consistent with the absence of glucose dependence in cross-linking (**Fig. 2a**) as well as with the distinct GK kinetic profiles of RO0281675 as compared to BAD SAHBs (**Table 1**).

In the absence of glucose, GK adopts an inactive super-open conformation (PDB 1V4T[10]), whereas in the presence of glucose, two distinct active structures have been reported: an active closed structure[10] and a glucose-bound intermediate structure[12] (PDB 1V4S[10] and 4DCH[12], respectively). On the basis of cross-linking of

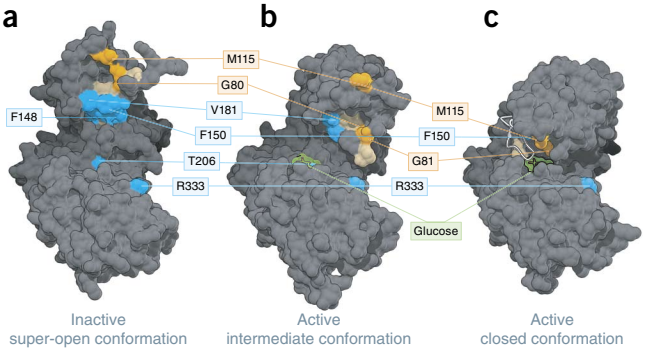

Figure 3 Mapping the phospho-BAD BH3 helix at the GK interaction site. (**a**–**c**) Phospho-BAD BH3 peptides bind to residues in the small domain of the inactive super-open and the active intermediate conformations, with the N terminus localized around residue M115 and the C terminus oriented toward residues V181, T206 and R333. The most frequently cross-linked residues for each BAD SAHB (≥25% threshold) are mapped onto the inactive super-open (**a**), active intermediate (**b**) and active closed (**c**) conformers of GK. Residues selectively cross-linked by BAD $SAHB_A$ (Y110Bpa S118pS) and (S118pS D123R F125Bpa) are colored orange and blue, respectively, and residues cross-linked by both photoreactive BAD SAHBs are colored tan. For clarity, all of the associated residues are colored, but not all are labeled. Cross-linked residues common to both peptides are among those listed in **Supplementary Table 3**. Glucose is depicted in green, the active site loop in white.

photoreactive BAD $SAHB_A$ compounds to a host of surface residues that would otherwise be buried in the active closed conformation, the mapped binding-site data are more consistent with phospho-BAD BH3 engagement of a structure that resembles the published inactive super-open or the active intermediate conformations of GK[10,12] (**Fig. 2d**,**e**). Furthermore, mapping of the most frequently cross-linked residues for each BAD $SAHB_A$ (≥25% threshold) onto each of the three GK structures suggests a discrete orientation for phospho-BAD BH3 at the binding interface (**Fig. 3**). In the context of the inactive super-open and the active intermediate conformations, phospho-BAD BH3 appears to almost exclusively engage the small domain, with the N terminus oriented toward M115 and the C terminus toward V181, T206 and R333 (**Fig. 3a**,**b**). In contrast, when mapped to the active closed conformer, the N terminus continues to localize to the M115 region of the small domain, but the C terminus would be capable of engaging only the exposed R333 residue of the large domain (**Fig. 3c**). Taken together, these data indicate that the phospho-BAD BH3 helix directly engages GK at a new interaction site that is distinct from that of small-molecule allosteric GKAs, results consistent with the unique modulatory effect of BAD observed on GK enzyme kinetics (**Table 1**).

Effect of the phospho-BAD BH3 helix on human donor islets

We previously have shown that phospho-BAD BH3 stapled peptides can restore the insulin-secretory defect of BAD-deficient mouse islets treated with stimulatory glucose concentrations[22]. However, the capacity of these compounds to further enhance insulin release in the presence of endogenous wild-type BAD has not previously been tested. Importantly, we sought to expand our efficacy testing of phospho-BAD SAHBs to human islets. We treated human islets overnight with 3 μM BAD $SAHB_A$ (S118D) or $SAHB_A$ (S118L) and assessed insulin release after incubation with basal (1.67 mM) or stimulatory (20 mM) glucose concentrations. At 20 mM glucose, islets pretreated with BAD $SAHB_A$ (S118D) showed a marked increase in insulin release, whereas islets pretreated with BAD $SAHB_A$ (S118L) secreted comparable levels of insulin to those of vehicle-treated control islets (**Fig. 4a**). The distinct capacities of BAD $SAHB_A$ (S118D) and $SAHB_A$ (S118L) to stimulate insulin secretion paralleled their effects on GK activation (**Table 1**). Importantly, pretreatment with BAD $SAHB_A$ did not augment insulin secretion at 1.67 mM glucose (**Fig. 4a**), a concentration that is insufficient to trigger GK activation. Collectively, these data indicate that direct modulation of GK activity by BAD $SAHB_A$ (S118D) augments glucose-stimulated insulin secretion, a specific functional outcome in human islets.

Kinetics of GK mutants treated with phospho-BAD mimetic

The location of the BAD $SAHB_A$ binding interface near the active site of GK prompted us to examine whether BAD SAHBs could alter the function of active site GK mutants, perhaps by stabilizing otherwise impaired structures, or whether these mutations might prevent BAD $SAHB_A$ binding altogether. GKAs can be expected to promote the protein stability of GK mutants in addition to increasing their activity[34]. We selected two naturally occurring MODY2 mutations located near the active site, M298K and E300K, for analysis[35–39]. Both mutations render the enzyme highly unstable[8,39,40]. Previous reports on the M298K mutation have noted substantial deficiencies in multiple enzymatic parameters[34,36,39,41]. We observed impaired kinetic constants for this mutant, including decreased V_{max}, diminished glucose affinity and a decreased Hill coefficient (**Fig. 4b** and **Table 2**), in agreement with these reports. Upon treatment with BAD $SAHB_A$ (S118D), these three kinetic parameters showed marked improvement, including restoration of V_{max} from 57% to 95% of that of the wild-type enzyme (**Fig. 4b** and **Table 2**). A similar series of studies using the M298K mutant in the presence of an allosteric GKA

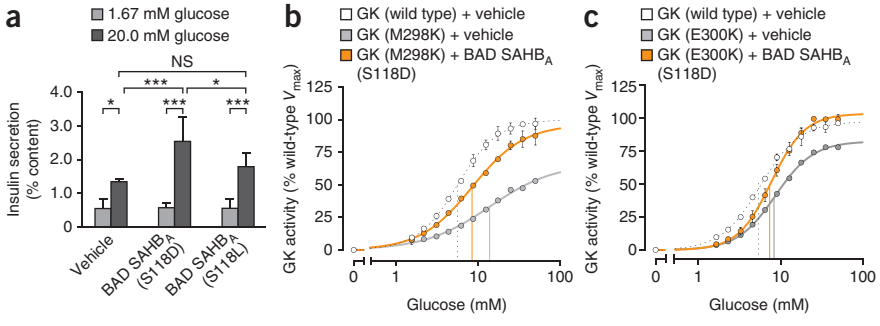

Figure 4 Effects of BAD BH3 stapled peptides on human islet function and human GK mutations. (**a**) Stimulation of insulin release by glucose in donor islets treated with BAD BH3 stapled peptides. Data are shown as means ± s.e.m. $*P < 0.05$; $***P < 0.001$; NS, not significant (two-way ANOVA). (**b**,**c**) Effects of BAD $SAHB_A$ (S118D) on the activity of GK active site mutations. Kinetic analyses of two human GK mutants, M298K (**b**) and E300K (**c**), in the absence or presence of BAD $SAHB_A$ (S118D). Wild-type human GK treated with vehicle was included in each assay as a control. Vertical lines indicate the glucose concentration corresponding to the $S_{0.5}$ obtained from the representative experiment shown. The data in **b** and **c** show means and range from representative experiments. **Table 2** summarizes all independent experiments performed similarly (four experiments per GK mutant).

Table 2 Enhancement of GK activity by phosphomimic BAD BH3 in select MODY2 mutations

Treatment	$S_{0.5}$ (mM)	V_{max} (% WT V_{max})	n_H	
GK (wild type) + vehicle	5.60 ± 0.06	100	1.73 ± 0.03	$n = 8$
GK (M298K) + vehicle	11.3 ± 0.90***	57.1 ± 4.02***	1.24 ± 0.05***	$n = 4$
GK (M298K) + BAD $SAHB_A$ (S118D)	8.08 ± 0.57†††	95.7 ± 9.47†††	1.43 ± 0.04†	$n = 4$
GK (E300K) + vehicle	8.39 ± 0.12***	84.3 ± 1.89*	1.83 ± 0.03	$n = 4$
GK (E300K) + BAD $SAHB_A$ (S118D)	8.02 ± 0.38	103 ± 8.35†	2.11 ± 0.08††	$n = 4$

Kinetic parameters were derived with the Hill equation. Data represent means ± s.e.m.
*$P < 0.05$; ***$P < 0.001$ compared with vehicle-treated recombinant human wild-type (WT) GK.
†$P < 0.05$; ††$P < 0.01$; †††$P < 0.001$ compared with vehicle-treated mutant GK by one-way ANOVA.

treatment reported a V_{max} increase from approximately 60% to 79% of that of wild-type[34]. However, the restoration of V_{max} in the presence of BAD $SAHB_A$ (S118D) occurred with modest effects on the $S_{0.5}$ of this mutant, which changed from approximately 11 mM to near-normal values of 8 mM (**Table 2**). This result was considerably different from the drastic lowering of $S_{0.5}$ to approximately 1 mM observed upon treatment of M298K with an allosteric GKA[34]. These findings reinforce the mechanistic distinction between allosteric GKAs and $SAHB_A$ (S118D) (**Table 1**).

The active site mutant E300K has previously been reported to display variable kinetics. Some studies indicate near-normal kinetics[36,37], whereas others have documented more-moderate and even severe[8,38] changes in the kinetic profile. We observed near-normal n_H and $S_{0.5}$ values but a noticeable decrease in V_{max} (84.3% ± 1.89 that of wild-type GK), results comparable to previous reports by Davis *et al.*[8] and Kesavan *et al.*[37]. Moreover, this mutant had low expression levels as previously reported[8,35,37,40]. Addition of BAD $SAHB_A$ (S118D) fully restored the V_{max} of this mutant to wild-type levels (**Fig. 4c** and **Table 2**). These data suggest that binding of BAD $SAHB_A$ (S118D) in the vicinity of the active site stabilizes the M298K and E300K mutant forms of GK, thus markedly improving their enzymatic function.

DISCUSSION

Our biochemical and structural dissection of the interaction between GK and the phospho-BAD BH3 helix demonstrates a new binding region and distinct mode of enzyme activation compared to those of allosteric GKAs. Binding of the BAD BH3 helix near the active site of GK augments V_{max} while preserving the native n_H and $S_{0.5}$ values. The relevance of this interaction mode is further underscored by the ability of the BAD BH3 helix to restore the function of two independent MODY2 mutations residing near the active site of GK. Direct engagement and activation of GK by the BAD BH3 helix also imparts a functional benefit to human donor islets, thus warranting exploration of BAD BH3 mimetic compounds as a new class of GKAs.

The positive cooperativity of monomeric GK for glucose is central to its role as a glucose sensor. This has been explained at the mechanistic level by the ligand-induced slow transition model[42] or the mnemonic model[10], which has been further refined as the pre-existing equilibrium model[12,13,16,32], all involving distinct conformations of GK, with different affinities for glucose, that interconvert slowly. Structural information for several GK conformers corroborates the mechanistic properties of the enzyme and the glucose dose-dependent conversion between conformations[7–11,13–16]. GK exists in a super-open conformation in low glucose concentrations and transitions to an active closed conformation in the presence of glucose and allosteric activators[10]. A glucose-bound intermediate conformation between the inactive super-open and the active closed conformers of GK was recently described[12]. It has been suggested that the degree to which allosteric activators enlarge the allosteric site may determine the extent to which the active site is closed and the affinity for glucose is increased[12]. The transition from this active intermediate to the active closed form is thought to allow higher-affinity glucose binding at the active site, thus enabling catalytic activity[12]. Given the inherent mobility of GK, it is likely that the spectrum of GK conformations in the presence or absence of glucose and other ligands will continue to expand[11,12] and provide new information on the mechanism of enzyme action.

The BAD BH3 domain is the minimal region required for BAD's capacity to activate GK and stimulate glucose metabolism[22]. Our integrative dissection of the mode of engagement and activation of GK by stapled peptides modeled after the BAD BH3 domain indicates that they directly bind GK in the immediate vicinity of the active site and activate the enzyme through a mechanism that is markedly distinct from that of all known allosteric activators, as evidenced by minimal alterations in the enzyme's affinity for glucose. To our knowledge, BAD BH3 mimetic compounds constitute the first example of synthetic GKAs exhibiting a nonallosteric mode of action.

Cross-linking patterns of the phospho-BAD BH3 helix on GK are largely unaffected by the presence or absence of either glucose or an allosteric GKA, both of which dramatically shift GK conformational equilibrium away from the inactive super-open conformation. MS-based mapping of the amino acids most frequently cross-linked by photoreactive BAD SAHBs onto published GK structures suggests that the conformation of BAD SAHB-bound GK probably resembles a structure similar to the inactive super-open or the active intermediate conformers in which the N terminus of the BAD BH3 domain solely engages the apex of the small domain of GK, and the C terminus binds near the interface between the small and large domains proximal to the glucose-binding site (**Fig. 3**). Several reports have proposed multiple intermediate GK conformations on the basis of tryptophan fluorescence[7,13,34,43,44], X-ray scattering[12] and NMR spectroscopy[45]. Such conformational dynamics were decreased, but not eliminated, in the presence of high glucose concentrations[45]. Thus, the explicit conformational structure of GK upon BAD BH3-domain engagement may indeed be distinct from the crystal structures published to date. Although the spectrum of GK conformers limits mechanistic interpretation of the activating nature of the BAD BH3 helix bound to GK, our data firmly place the BAD BH3 domain near the active site of the enzyme. As a result of this direct interaction, the BAD BH3 domain may stabilize and enable conformational transitions of GK facilitating catalysis or enhancing release of products. This scenario would be consistent with the functional restoration of the M298K and E300K active site mutants in the presence of BAD $SAHB_A$ (S118D).

GK activating mutations predominantly cluster in the allosteric site and lower the $S_{0.5}$ of the enzyme[5,39,46,47]. The residues identified in our cross-linking studies tend to be closer to a region between the small and large domains of GK than are any of the residues associated with GK activating mutations reported to date, which largely exist away from the glucose-binding site and the proposed BAD interface. Among residues altered in GK activating mutations, V452 is closest to any of those proposed within the interface between GK and the BAD BH3 helix in the inactive open conformation and active intermediate conformation. However, the kinetic profile of the corresponding activating mutation, V452L, differs greatly from the kinetic profiles we have observed in the presence of BAD SAHBs[34]. In light of these considerations and the results of our binding-site localization studies,

it appears that the interface between GK and the BAD BH3 helix is independent from the locations of the known GK activating mutations.

To date, all published small-molecule GKAs markedly increase the affinity of the enzyme for glucose[9,10,14,15,17,19,27,30]. This is similar to kinetic alterations reported for GK activating mutations in persistent hyperinsulinemic hypoglycemia of infancy[5,39,46,47]. Beyond their shared capacity to augment the affinity of GK for glucose, GKAs can have diverse effects on the substrate cooperativity and V_{max} of the enzyme[5]. Several studies examining the short-term effects of allosteric GKAs (less than one week) in human subjects with early T2D have reported promising outcomes, including improved β-cell function, decreased hepatic glucose output and a net lowering of glucose levels in glucose tolerance tests that are consistent with known physiologic roles of GK in the β-cell and in liver[17,18]. However, a concern with allosteric GKAs is their ability to decrease the glucose threshold for GK activation, thus resulting in marked glucose-lowering capacity and the risk of hypoglycemia, as well as other undesired effects such as increased triglyceride levels[19]. This latter effect is expected upon chronic activation of hepatic GK and the associated stimulation of lipogenesis and increased hepatic fat content[48–50]. Lower doses of GKAs or combination therapies with other antidiabetic agents may circumvent these undesirable outcomes[5]. Furthermore, studies that tested the long-term effects of certain allosteric GKAs (up to four months) in T2D subjects reported initial improvement of glucose homeostasis with a loss of efficacy over time that is not fully understood[19,51,52]. These complications are also relevant if pharmacologic activation of GK is to be used as a potential therapeutic approach for expansion of functional β-cell mass in T1D[6].

The successes and challenges of allosteric GKAs in T2D therapy have spurred active investigation of other chemical and enzymatic modes of GK activation, including development of different classes of GKAs that preserve the native enzymatic properties of the enzyme, especially its affinity for glucose[5], or 'partial agonists' that more moderately lower the $S_{0.5}$ for glucose[12]. To our knowledge, BAD SAHBs are the first example of a class of synthetic GKAs that raise the V_{max} with minimal effect on the affinity of the enzyme for glucose. This is mediated by engaging the enzyme near its active site, thus revealing a new druggable site on GK. By preserving the natural kinetic properties of GK, compounds modeled after the phospho-BAD BH3 helix may have important therapeutic benefits, in addition to serving as powerful tool compounds for further biophysical, structural and enzymatic dissection of GK and its pathologic mutants.

METHODS

Methods and any associated references are available in the online version of the paper.

Note: Any Supplementary Information and Source Data files are available in the online version of the paper.

ACKNOWLEDGMENTS

We thank K. Robertson and P. Chen for technical assistance; F. Bernal, S. Devarakonda and C. Buettger for advice on protein purification; E. Gavathiotis, A. West and R. McNally for advice on structural studies; and M. Eck, N. Gray, S. Blacklow, G. Yellen and members of the Danial and Walensky laboratories for valuable discussions. This work was supported by US National Institutes of Health grants R01DK078081 (N.N.D.) and R01GM090299 (L.D.W.), a Burroughs Wellcome Fund Career Award in Biomedical Sciences (N.N.D.), Juvenile Diabetes Research Foundation grant 17-2011-595 (N.N.D.), a Claudia Adams Barr Award in Innovative Basic Cancer Research (N.N.D.), a Stand Up to Cancer Innovative Research Grant (L.D.W.), a National Sciences and Engineering Research Council of Canada postgraduate scholarship (C.R.B.), a Swiss National Science Foundation postdoctoral fellowship (S.L.) and a Juvenile Diabetes Research Foundation postdoctoral fellowship (M.A.O.).

AUTHOR CONTRIBUTIONS

B.S., E.P., M.A.O. and N.N.D. purified recombinant proteins and performed enzyme kinetic analyses. C.R.B., G.H.B. and L.D.W. designed, synthesized and characterized SAHB compounds. C.R.B. and L.D.W. performed cross-linking, MS and structural analyses. S.L. and N.N.D. performed analyses in human donor islets. B.S., C.R.B., L.D.W. and N.N.D. wrote the manuscript. F.M.M. provided critical advice and reviewed the manuscript.

COMPETING FINANCIAL INTERESTS

The authors declare competing financial interests: details are available in the online version of the paper.

1. Ashcroft, F.M. & Rorsman, P. Diabetes mellitus and the β cell: the last ten years. *Cell* **148**, 1160–1171 (2012).
2. Samuel, V.T. & Shulman, G.I. Mechanisms for insulin resistance: common threads and missing links. *Cell* **148**, 852–871 (2012).
3. Majumdar, S.K. & Inzucchi, S.E. Investigational anti-hyperglycemic agents: the future of type 2 diabetes therapy? *Endocrine* **44**, 47–58 (2013).
4. Grimsby, J., Berthel, S.J. & Sarabu, R. Glucokinase activators for the potential treatment of type 2 diabetes. *Curr. Top. Med. Chem.* **8**, 1524–1532 (2008).
5. Matschinsky, F.M. Assessing the potential of glucokinase activators in diabetes therapy. *Nat. Rev. Drug Discov.* **8**, 399–416 (2009).
6. Dadon, D. *et al.* Glucose metabolism: key endogenous regulator of β-cell replication and survival. *Diabetes Obes. Metab.* **14** (suppl. 3), 101–108 (2012).
7. Antoine, M., Boutin, J.A. & Ferry, G. Binding kinetics of glucose and allosteric activators to human glucokinase reveal multiple conformational states. *Biochemistry* **48**, 5466–5482 (2009).
8. Davis, E.A. *et al.* Mutants of glucokinase cause hypoglycaemia- and hyperglycaemia syndromes and their analysis illuminates fundamental quantitative concepts of glucose homeostasis. *Diabetologia* **42**, 1175–1186 (1999).
9. Grimsby, J. *et al.* Allosteric activators of glucokinase: potential role in diabetes therapy. *Science* **301**, 370–373 (2003).
10. Kamata, K., Mitsuya, M., Nishimura, T., Eiki, J. & Nagata, Y. Structural basis for allosteric regulation of the monomeric allosteric enzyme human glucokinase. *Structure* **12**, 429–438 (2004).
11. Larion, M., Salinas, R.K., Bruschweiler-Li, L., Bruschweiler, R. & Miller, B.G. Direct evidence of conformational heterogeneity in human pancreatic glucokinase from high-resolution nuclear magnetic resonance. *Biochemistry* **49**, 7969–7971 (2010).
12. Liu, S. *et al.* Insights into mechanism of glucokinase activation: observation of multiple distinct protein conformations. *J. Biol. Chem.* **287**, 13598–13610 (2012).
13. Petit, P. *et al.* The active conformation of human glucokinase is not altered by allosteric activators. *Acta Crystallogr. D Biol. Crystallogr.* **67**, 929–935 (2011).
14. Pfefferkorn, J.A. *et al.* Discovery of (*S*)-6-(3-cyclopentyl-2-(4-(trifluoromethyl)-1H-imidazol-1-yl)propanamido)nicotinic acid as a hepatoselective glucokinase activator clinical candidate for treating type 2 diabetes mellitus. *J. Med. Chem.* **55**, 1318–1333 (2012).
15. Futamura, M. *et al.* An allosteric activator of glucokinase impairs the interaction of glucokinase and glucokinase regulatory protein and regulates glucose metabolism. *J. Biol. Chem.* **281**, 37668–37674 (2006).
16. Pfefferkorn, J.A. *et al.* Pyridones as glucokinase activators: identification of a unique metabolic liability of the 4-sulfonyl-2-pyridone heterocycle. *Bioorg. Med. Chem. Lett.* **19**, 3247–3252 (2009).
17. Bonadonna, R.C. *et al.* Piragliatin (RO4389620), a novel glucokinase activator, lowers plasma glucose both in the postabsorptive state and after a glucose challenge in patients with type 2 diabetes mellitus: a mechanistic study. *J. Clin. Endocrinol. Metab.* **95**, 5028–5036 (2010).
18. Ericsson, H. *et al.* Tolerability, pharmacokinetics, and pharmacodynamics of the glucokinase activator AZD1656, after single ascending doses in healthy subjects during euglycemic clamp. *Int. J. Clin. Pharmacol. Ther.* **50**, 765–777 (2012).
19. Meininger, G.E. *et al.* Effects of MK-0941, a novel glucokinase activator, on glycemic control in insulin-treated patients with type 2 diabetes. *Diabetes Care* **34**, 2560–2566 (2011).
20. Danial, N.N. BAD: undertaker by night, candyman by day. *Oncogene* **27** (suppl. 1), S53–S70 (2008).
21. Danial, N.N. *et al.* BAD and glucokinase reside in a mitochondrial complex that integrates glycolysis and apoptosis. *Nature* **424**, 952–956 (2003).
22. Danial, N.N. *et al.* Dual role of proapoptotic BAD in insulin secretion and beta cell survival. *Nat. Med.* **14**, 144–153 (2008).
23. Liu, S. *et al.* Insulin signaling regulates mitochondrial function in pancreatic β-cells. *PLoS ONE* **4**, e7983 (2009).
24. Gavathiotis, E. *et al.* BAX activation is initiated at a novel interaction site. *Nature* **455**, 1076–1081 (2008).

25. LaBelle, J.L. *et al.* A stapled BIM peptide overcomes apoptotic resistance in hematologic cancers. *J. Clin. Invest.* **122**, 2018–2031 (2012).
26. Leshchiner, E.S., Braun, C.R., Bird, G.H. & Walensky, L.D. Direct activation of full-length proapoptotic BAK. *Proc. Natl. Acad. Sci. USA* **110**, E986–E995 (2013).
27. Bebernitz, G.R. *et al.* Investigation of functionally liver selective glucokinase activators for the treatment of type 2 diabetes. *J. Med. Chem.* **52**, 6142–6152 (2009).
28. Brocklehurst, K.J. *et al.* Stimulation of hepatocyte glucose metabolism by novel small molecule glucokinase activators. *Diabetes* **53**, 535–541 (2004).
29. Castelhano, A.L. *et al.* Glucokinase-activating ureas. *Bioorg. Med. Chem. Lett.* **15**, 1501–1504 (2005).
30. Efanov, A.M. *et al.* A novel glucokinase activator modulates pancreatic islet and hepatocyte function. *Endocrinology* **146**, 3696–3701 (2005).
31. Fyfe, M.C. *et al.* Glucokinase activator PSN-GK1 displays enhanced antihyperglycaemic and insulinotropic actions. *Diabetologia* **50**, 1277–1287 (2007).
32. Ralph, E.C., Thomson, J., Almaden, J. & Sun, S. Glucose modulation of glucokinase activation by small molecules. *Biochemistry* **47**, 5028–5036 (2008).
33. Braun, C.R. *et al.* Photoreactive stapled BH3 peptides to dissect the BCL-2 family interactome. *Chem. Biol.* **17**, 1325–1333 (2010).
34. Zelent, B. *et al.* Mutational analysis of allosteric activation and inhibition of glucokinase. *Biochem. J.* **440**, 203–215 (2011).
35. Gidh-Jain, M. *et al.* Glucokinase mutations associated with non-insulin-dependent (type 2) diabetes mellitus have decreased enzymatic activity: implications for structure/function relationships. *Proc. Natl. Acad. Sci. USA* **90**, 1932–1936 (1993).
36. Gloyn, A. *et al.* in *Glucokinase and Glycemic Diseases: From the Basics to Novel Therapeutics* (eds. Matschinsky, F.M. & Magnuson, M.A.) 92–109 (Karger, Basel, 2004).
37. Kesavan, P. *et al.* Structural instability of mutant β-cell glucokinase: implications for the molecular pathogenesis of maturity-onset diabetes of the young (type-2). *Biochem. J.* **322**, 57–63 (1997).
38. Liang, Y. *et al.* Variable effects of maturity-onset-diabetes-of-youth (MODY)-associated glucokinase mutations on substrate interactions and stability of the enzyme. *Biochem. J.* **309**, 167–173 (1995).
39. Osbak, K.K. *et al.* Update on mutations in glucokinase (GCK), which cause maturity-onset diabetes of the young, permanent neonatal diabetes, and hyperinsulinemic hypoglycemia. *Hum. Mutat.* **30**, 1512–1526 (2009).
40. Cullen, K.S., Matschinsky, F.M., Agius, L. & Arden, C. Susceptibility of glucokinase-MODY mutants to inactivation by oxidative stress in pancreatic β-cells. *Diabetes* **60**, 3175–3185 (2011).
41. Barrio, R. *et al.* Nine novel mutations in maturity-onset diabetes of the young (MODY) candidate genes in 22 Spanish families. *J. Clin. Endocrinol. Metab.* **87**, 2532–2539 (2002).
42. Larion, M. & Miller, B.G. Global fit analysis of glucose binding curves reveals a minimal model for kinetic cooperativity in human glucokinase. *Biochemistry* **49**, 8902–8911 (2010).
43. Lin, S.X. & Neet, K.E. Demonstration of a slow conformational change in liver glucokinase by fluorescence spectroscopy. *J. Biol. Chem.* **265**, 9670–9675 (1990).
44. Molnes, J., Bjorkhaug, L., Sovik, O., Njolstad, P.R. & Flatmark, T. Catalytic activation of human glucokinase by substrate binding: residue contacts involved in the binding of D-glucose to the super-open form and conformational transitions. *FEBS J.* **275**, 2467–2481 (2008).
45. Larion, M. & Miller, B.G. Homotropic allosteric regulation in monomeric mammalian glucokinase. *Arch. Biochem. Biophys.* **519**, 103–111 (2012).
46. Barbetti, F. *et al.* Opposite clinical phenotypes of glucokinase disease: description of a novel activating mutation and contiguous inactivating mutations in human glucokinase (*GCK*) gene. *Mol. Endocrinol.* **23**, 1983–1989 (2009).
47. Kassem, S. *et al.* Large islets, beta-cell proliferation, and a glucokinase mutation. *N. Engl. J. Med.* **362**, 1348–1350 (2010).
48. Ferre, T., Riu, E., Franckhauser, S., Agudo, J. & Bosch, F. Long-term overexpression of glucokinase in the liver of transgenic mice leads to insulin resistance. *Diabetologia* **46**, 1662–1668 (2003).
49. O'Doherty, R.M., Lehman, D.L., Telemaque-Potts, S. & Newgard, C.B. Metabolic impact of glucokinase overexpression in liver: lowering of blood glucose in fed rats is accompanied by hyperlipidemia. *Diabetes* **48**, 2022–2027 (1999).
50. Peter, A. *et al.* Hepatic glucokinase expression is associated with lipogenesis and fatty liver in humans. *J. Clin. Endocrinol. Metab.* **96**, E1126–E1130 (2011).
51. Kiyosue, A., Hayashi, N., Komori, H., Leonsson-Zachrisson, M. & Johnsson, E. Dose-ranging study with the glucokinase activator AZD1656 as monotherapy in Japanese patients with type 2 diabetes mellitus. *Diabetes Obes. Metab.* **15**, 923–930 (2013).
52. Wilding, J.P., Leonsson-Zachrisson, M., Wessman, C. & Johnsson, E. Dose-ranging study with the glucokinase activator AZD1656 in patients with type 2 diabetes mellitus on metformin. *Diabetes Obes. Metab.* **15**, 750–759 (2013).

ONLINE METHODS

Recombinant GK expression and purification. Mouse GK isoform 1 was cloned in the pET-43.1 Ek/LIC vector (Novagen) containing an N-terminal hexahistidine tag that was further engineered to express a TEV cleavage site (ENLYFQS) preceding the GK sequence. The resultant recombinant GK was purified as follows and used in experiments (**Figs. 1–3**, **Table 1** and **Supplementary Tables 2** and **3**). Briefly, *Escherichia coli* BL21(DE3) pLysS transformed with the construct were grown at 37 °C to an optical density of 0.5–0.6 at 595 nm, and the expression of GK fusion protein was induced with 0.6 mM IPTG for 6 h at 30 °C. The cells were harvested, resuspended in 100 mM sodium phosphate, pH 7.4, 500 mM NaCl, 5 mM BME, 1 mM PMSF and EDTA-free complete protease inhibitor cocktail (Roche), and sonicated at 4 °C (Misonix, Inc. S-4000). The lysates were passed over a Ni-NTA agarose matrix (Qiagen), and ion-exchange chromatography was performed with a Mono Q 5/50 GL (GE Life Sciences) with a NaCl gradient and gel filtration with a Superdex 75 10/300 GL column (GE Life Sciences) in 50 mM Tris, 150 mM NaCl and 5 mM DTT, pH 7.4. Aliquots of purified GK were stored at –80 °C with 20% glycerol (v/v).

N-terminal GST-tagged constructs (pGEX3) expressing the recombinant human wild-type GK isoform 1 and the M298K and E300K GK active site mutations (used in **Fig. 4** and **Table 2**) have been previously described[37,38]. Briefly, BL21(DE3) transformed with the constructs were induced with IPTG overnight at 25 °C and lysed in buffer containing 4 mM KH_2PO_4, 16 mM K_2HPO_4, 150 mM KCl and 5 mM DTT as previously described[38]. Tagged GST-hGK was captured with glutathione agarose beads (Sigma), cleaved on column by incubation with Factor Xa (GE Life Sciences), and subjected to gel filtration.

SAHB synthesis. Peptide synthesis, olefin metathesis, N-terminal derivatization (for example, biotin-βAla), reverse-phase HPLC purification, and amino acid analysis were performed as previously described[22,33].

Steady-state kinetics. Glucokinase activity was measured by monitoring of the rate of NADH formation with a G6PDH-coupled reaction as previously described[38], with minor modifications. Briefly, assays were performed at 37 °C in 100 µL total volume per well of a Costar 3596 plate with a SpectraMax M5 microplate reader (Molecular Devices). Absorbance at 340 nm was recorded every 2 min, and the change in absorbance per minute was calculated with data between 30 and 60 min, where the rate of reaction was linear. Reaction wells were prepared on ice and contained final concentrations of 7.5 nM GK, 100 mM HEPES, pH 7.4, 150 mM KCl, 6 mM $MgCl_2$, 1 mM DTT, 1 mM NAD, 0.05% BSA, 2.5 units G6PDH and 5% DMSO in the presence or absence of 5 µM BAD SAHBs (a concentration deemed near saturating on the basis of dose-response assays) and/or 3 µM of RO0281675 (Axon Medchem BV). To determine glucose-dependent kinetic parameters, glucose was varied (0–50 mM) while ATP was maintained at 5 mM. Kinetic parameters were derived from the Hill equation with GraphPad Prism 6.0a.

Cross-linking of photoreactive BAD SAHBs and glucokinase. Photoreactive BAD SAHBs were applied in protein target cross-linking as previously reported[33]. Briefly, SAHBs (10 µM) containing benzophenone moieties were mixed with recombinant mouse glucokinase (5 µM) in buffer A (50 mM Tris, 5 mM DTT and 200 mM NaCl, pH 7.5) with or without the addition of 50 mM glucose as indicated, incubated for 15 min, and then irradiated with UV light (365 nm) for 2 h on ice. Unreacted SAHBs were removed by dialysis overnight at 4 °C in buffer B (50 mM Tris, 200 mM NaCl, pH 7.5) with 6–8 kDa MWCO D-tube dialyzers (EMD Biosciences). Cross-linking in the presence of RO0281675 was performed with 50 mM glucose and 3 µM RO0281675. Biotin affinity capture, elution, and gel electrophoresis were performed as described[33].

Western analysis of photoaffinity-captured proteins. After electrophoresis and transfer to PDVF, membranes were blocked in PBS containing 5% milk for 30 min at room temperature. The membranes were rinsed with PBS containing 3% bovine serum albumin (BSA) and subsequently probed with purified goat anti-biotin antibody conjugated to horseradish peroxidase (Cell Signaling Technology, 7075) at a dilution of 1:1,000 in PBS containing 3% BSA overnight as previously described[33]. After three washes for 15 min with PBS containing 0.1% Tween-20, bands were detected by chemiluminescence (PerkinElmer).

Mass spectrometry analysis. Samples were subjected to in-gel digestion and MS as described[33]. Searches were done with the sequest algorithm[53], with a sequence-reversed search database composed of GK, trypsin, and common keratin contaminants. Search results were limited to those peptides containing a BAD SAHB cross-linked adduct. False-positive identifications (considered to be any cross-linked peptides derived from trypsin or keratins, from the reversed database, or from peptides with masses corresponding to more than one cross-linked adduct) were limited to less than 5% via linear discriminant analysis of multiple variables including mass accuracy, XCorr, tryptic state, and charge state. MS/MS spectral counting was performed as described[33]. Spectral counts for cross-linking to each residue were normalized in each experiment such that the most frequently detected residue was assigned a value of 100%, while 0% indicated no cross-linking. The normalized values for each experiment were then combined and averaged to generate frequency distribution plots. For **Figure 3**, a value of 25% for this normalized average frequency of spectral counts was chosen for depicting the differential cross-linking pattern of N- and C-terminal photoreactive BAD SAHBs. This 25% cutoff was chosen in accordance with observations from both published[26,33] and unreported experiments indicating that when crystal structures of an interaction are known, higher relative cross-linking frequency generally correlates with better agreement with these structures.

Human islet culture, SAHB treatment and insulin-release assays. Human donor islets were obtained through the Integrated Islet Distributing Program (http://iidp.coh.org/). Islets were cultured according to established protocols[54], at 37 °C (5% CO_2) in CMRL 1066 medium (Gibco) containing 5.5 mM glucose and supplemented with human albumin serum (10%, Gemini)[55], L-glutamine (2 mM, Sigma), HEPES (1 mM, Sigma), and 0.1% insulin-transferrin-selenium, pH 7.4. Islets were cultured at least an additional 24 h before treatment with 3 µM BAD SAHBs or vehicle (DMSO 0.3%) in CMRL 1066 medium containing 5.5 mM glucose, supplemented with 10% human serum, pH 6.2, overnight at 37 °C. Islets were then incubated for 90 min in basal conditions (1.67 mM glucose), hand-picked and incubated in either basal (1.67 mM glucose) or stimulatory glucose condition (20 mM glucose) for 45 min[54], and insulin secretion was measured as previously described[56].

Statistical analysis. Statistical significance was calculated in GraphPad Prism 6.0a (http://www.graphpad.com/) with one-way ANOVA and an appropriate post test. For determination of the effects of BAD SAHB compounds on wild-type GK activity (**Table 1** and **Supplementary Table 2**), comparisons were made with one-way ANOVA and a subsequent Dunnett's test with the vehicle data as the control in each case. For comparison of mutant GK activity in the absence or presence of BAD $SAHB_A$ (S118D) (**Table 2**), analyses used one-way ANOVA and a subsequent Holm-Šídák test involving four comparisons in total. For comparison of the effects of BAD SAHB compounds on insulin secretion in human islets, two-way ANOVA and a subsequent Tukey multiple comparisons test were used. For all analyses, thresholds for significance used multiplicity-adjusted *P* values to account for multiple comparisons.

53. Eng, J.K., McCormack, A.L. & Yates, J.R. An approach to correlate tandem mass spectral data of peptides with amino acid sequences in a protein database. *J. Am. Soc. Mass Spectrom.* **5**, 976–989 (1994).
54. Murdoch, T.B., McGhee-Wilson, D., Shapiro, A.M. & Lakey, J.R. Methods of human islet culture for transplantation. *Cell Transplant.* **13**, 605–617 (2004).
55. Barbaro, B. *et al.* Increased albumin concentration reduces apoptosis and improves functionality of human islets. *Artif. Cells Blood Substit. Immobil. Biotechnol.* **36**, 74–81 (2008).
56. Mahdi, T. *et al.* Secreted frizzled-related protein 4 reduces insulin secretion and is overexpressed in type 2 diabetes. *Cell Metab.* **16**, 625–633 (2012).

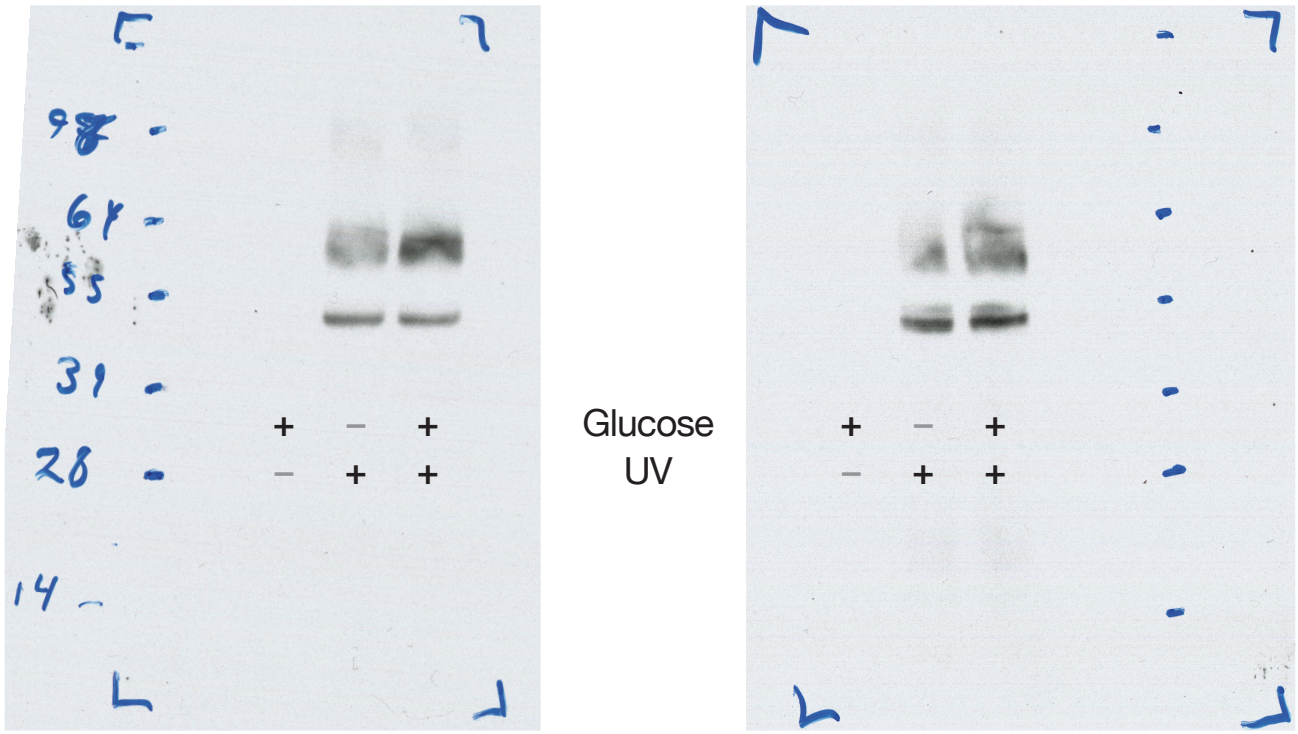

Supplementary Figure 1 Phospho-BAD BH3 peptides cross-link to GK after UV exposure in the presence or absence of glucose. Uncropped gels related to **Figure 2a** document detection of the BAD SAHB$_A$–GK cross-linked complex as visualized by western blot analysis using an anti-biotin antibody. The lower band corresponds to monomeric GK cross-linked to the BAD SAHB$_A$ compound, which was excised and subjected to MS/MS analysis.

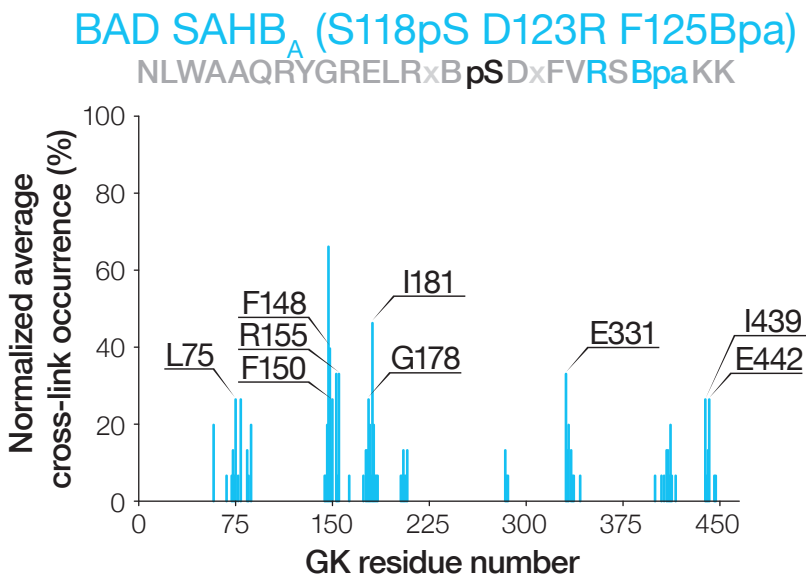

Supplementary Figure 2 Cross-linking profile of a BAD BH3 stapled peptide in the presence of glucose and RO0281675. Spectral count frequency of BAD SAHB$_A$ (S118pS D123R F125Bpa) crosslinked along the GK protein sequence. GK residues involved in cross-linking, which were unique to that peptide (with a frequency >25%), are labeled.

Peptide	N-term	Sequence	Applied in
BAD SAHB$_A$ (S118D)		NLWAAQRYGRELRXBDDXFVDSFKK	Fig. 1, 4, Table 1, 2
BAD SAHB$_A$ (S118L)		NLWAAQRYGRELRXBLDXFVDSFKK	Fig. 1, 4, Table 1
BAD SAHB$_A$ (S118pS)		NLWAAQRYGRELRXB$_p$SDXFVDSFKK	Table 1
BAD SAHB$_A$ (Y110Bpa S118pS)	Biotin-βala	NLWAAQRUGRELRXB$_p$SDXFVDSFKK	Fig. 2, 3, Supp. Fig. 1, Supp. Table 2, 3
BAD SAHB$_A$ (S118pS D123R F125Bpa)	Biotin-βala	NLWAAQRYGRELRXB$_p$SDXFVRSUKK	Fig. 2, 3, Supp. Fig. 1, 2, Supp. Table 2, 3
BAD SAHB$_A$ (S118D)	Biotin-βala	NLWAAQRYGRELRXBDDXFVDSFKK	Supp. Table 2

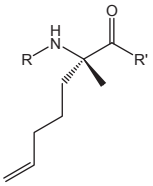

X : (S)-2-(4'-pentenyl) alanine

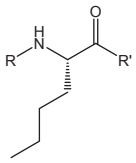

B : L-norleucine

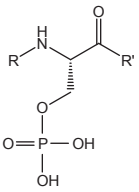

pS : phosphoserine

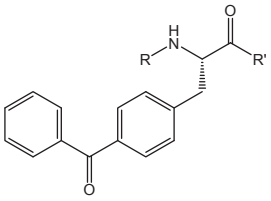

U : 4-benzoyl-L-phenylalanine (Bpa)

Supplementary Table 1 Composition of BAD BH3 stapled peptides. BAD BH3 compounds were synthesized as described in Online Methods. The N-termini of the peptides were acetylated unless otherwise stated. Residues in the protein sequence highlighted in green indicate substitutions from the wild-type sequence, while those in red denote changes to non-natural amino acids.

Treatment	$S_{0.5}$ (mM)	V_{max} (% veh.)	n_H	
Vehicle	8.35 ± 0.04	100	1.59 ± 0.03	(n = 3)
BAD $SAHB_A$ (S118D)	7.06 ± 0.42	144 ± 11.8 *	1.70 ± 0.06	(n = 3)
BAD $SAHB_A$ (Y110Bpa S118pS)	6.29 ± 0.34 *	152 ± 14.5 *	1.83 ± 0.06 *	(n = 3)
BAD $SAHB_A$ (S118pS D123R F125Bpa)	6.92 ± 0.51	122 ± 8.80	1.71 ± 0.06	(n = 3)

Supplementary Table 2 Summary of the effects of biotinylated BAD BH3 stapled peptides. Kinetic parameters were derived using the Hill equation as described in the Online Methods. Data represent means ± s.e.m. * $P < 0.05$ compared with vehicle control (one-way ANOVA).

a

BAD $SAHB_A$ (Y110Bpa S118pS)

GK residue	Mean frequency
G147	72%
L79	55%
M115	41%
G81	29%
D78	27%
G80	26%
P153	26%
T116	19%
A114	18%
E120	18%

b

BAD $SAHB_A$ (S118pS D123R F125Bpa)

GK residue	Mean frequency
P153	76%
G147	67%
I181	66%
F148	60%
R333	56%
F150	41%
L79	39%
G72	32%
L146	29%
T206	28%

Supplementary Table 3 Ten most-frequently captured GK residues involved in cross-linking with each photoreactive BAD BH3 stapled peptide. Normalized average frequency of phospho-BAD BH3 peptides derivitized with a 4-benzoyl-L-phenylalanine at either the N-terminus (**a**) or C-terminus (**b**).